SCIENTIFIC REPORTS

OPEN

SUBJECT AREAS:
BIOLOGICAL MOLECULES
DEVELOPMENT
NEUROANATOMY
NANOBIOTECHNOLOGY

Received
15 May 2012

Accepted
3 September 2012

Published
20 September 2012

Correspondence and requests for materials should be addressed to G.P. (pinato@iom.cnr.it) or D.C. (cojoc@iom.cnr.it) or V.T. (torre@sissa.it)

* These authors contributed equally.

Less than 5 Netrin-1 molecules initiate attraction but 200 Sema3A molecules are necessary for repulsion

Giulietta Pinato[1]*, Dan Cojoc[1]*, Linh Thuy Lien[2], Alessio Ansuini[2], Jelena Ban[2], Elisa D'Este[1] & Vincent Torre[2,3]

[1]Istituto Officina dei Materiali (IOM-CNR), Area Science Park, Basovizza, S.S. 14, Km 163.5, 34149 Trieste, Italy, [2]Neurobiology Sector, International School for Advanced Studies (SISSA), via Bonomea 265, 34136 Trieste, Italy, [3]IIT, Italian Institute of Technology, SISSA-Unit, Trieste, Italy.

Guidance molecules, such as Sema3A or Netrin-1, induce growth cone (GC) repulsion or attraction. In order to determine the speed of action and efficiency of these guidance cues we developed an experimental procedure to deliver controlled amounts of these molecules. Lipid vesicles encapsulating 10–10^4 molecules of Sema3A or Netrin-1 were manipulated with high spatial and temporal resolution by optical tweezers and their photolysis triggered by laser pulses. Guidance molecules released from the vesicles diffused and reached the GC membrane in a few seconds. Following their arrival, GCs retracted or grew in 20–120 s. By determining the number of guidance molecules trapped inside vesicles and estimating the fraction of guidance molecules reaching the GC, we show that the arrival of less than 5 Netrin-1 molecules on the GC membrane is sufficient to induce growth. In contrast, the arrival of about 200 Sema3A molecules is necessary to induce filopodia repulsion.

During development and in the adult brain, neurons continuously explore the environment searching for guidance cues, leading to the appropriate connections[1–4]. Growth cones (GCs) are the major motile structures involved in axon guidance[5–8] and are located at the neurite tips. GCs are composed of a lamellipodium from which thin filopodia emerge[9–12]. Filopodia exploratory motion is controlled and tuned by guidance molecules, which can attract or repel. Four main families of guidance molecules have been identified[13], such as Semaphorins[14], Netrins[15], Slits[16] and Ephrins[17]. The secreted protein Sema3A can cause a complete repulsion of the GC by inducing the depolymerization of the actin filament network inside the GC lamellipodium. Neuropilin-1 (NP1) and members of the class A plexins (PlexA) form a Sema3A receptor complex. Receptors for Netrin-1 are formed by a combination of deleted in colorectal cancer (DCC) proteins and UNC5 receptors[18,19] and their combination determines whether Netrin-1 mediates attraction or repulsion: homodimers of DCC proteins mediate attraction and heterodimers of DCC and UNC5 mediate repulsion[20]. Signaling pathways activated by Sema3A and Netrin-1 receptors require second messengers Ca^{2+} and cyclic nucleotides[21] activating GEFs and GAPs regulators of Rho family of small GTP-ases and various kinases. Rho GTP-ases coordinate downstream effects on cytoskeletal assembly[22]. These signaling pathways are not fully understood and very little is known on their speed and efficiency. The determination of the speed of action and of the minimum number of guidance molecules necessary to induce attraction or repulsion requires a precise control of the delivery of guidance molecules.

Recent techniques exploiting phospholipid vesicles as chemical microcontainers[23,24] allow the delivery of controlled amounts of molecules to living cells[25–27]. By optical manipulation of vesicles encapsulating Netrin-1 or Sema-3A we have achieved a fine control of the number of molecules reaching GCs of hippocampal neurons. Most importantly, our method provides an upper bound on the number of Sema3A and Netrin-1 molecules reaching their target, which can be as small as 5–200. In this way, we have determined two major dynamical properties of these signaling cascades: i - the lag between molecule arrival on the GC membrane and initiation of cytoskeleton remodeling; ii- the minimum number of Sema3A and Netrin-1 molecules necessary to initiate GC repulsion and growth.

Results

Sema3A and Netrin-1 solutions at different concentrations were encapsulated in lipid vesicles with a diameter varying between 1 and 5 μm (see Methods). By changing the concentration of Sema3A/Netrin-1, and the vesicle

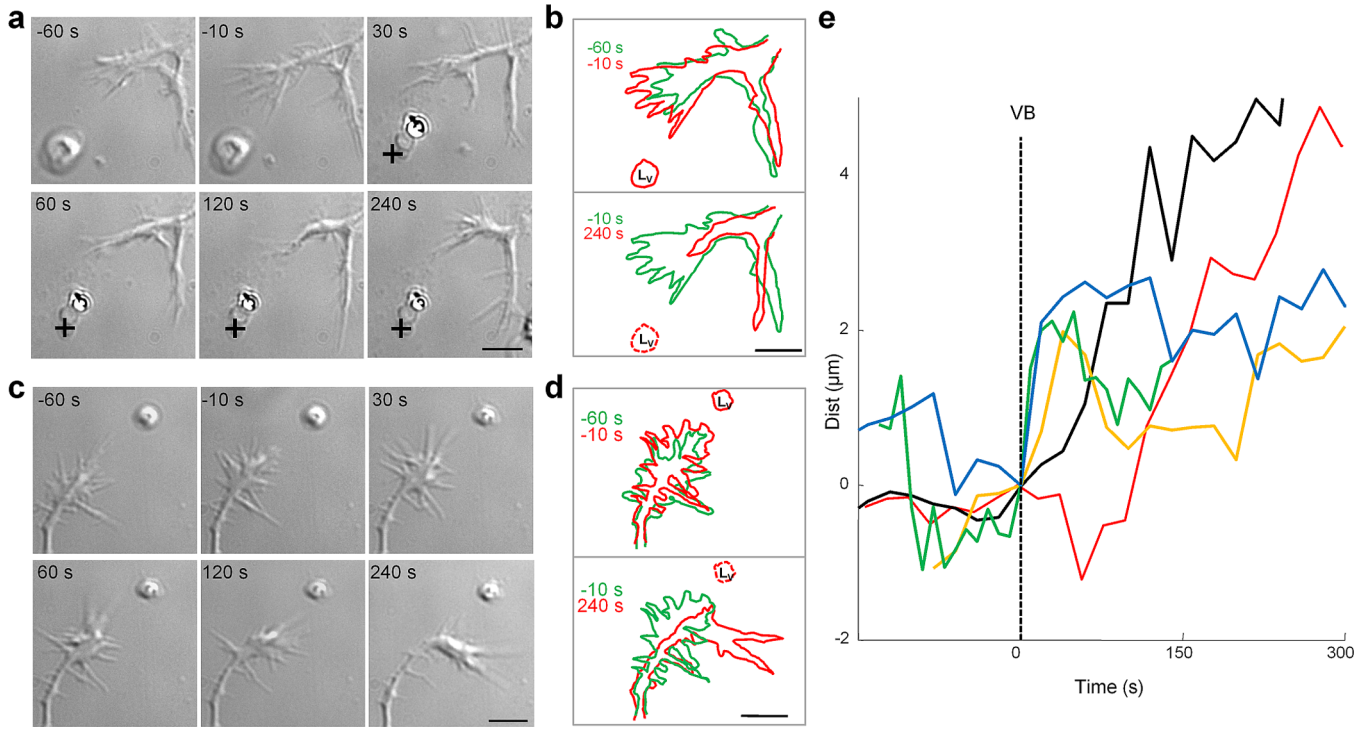

Figure 1 | The release of Sema3A from vesicles induces repulsion. (a) DIC images of a GC before VB (−60 s and −10 s) and after VB (30 s, 60 s, 120 s and 240 s). Black crosses indicate L_v. (b) top: GC profiles at −60 s (green) and −10 s (red) before VB; bottom: GC profiles at −10 s (green) and 240 s (red) after VB. Before VB the GC explored the environment, but after VB the GC quickly retracted. The estimated number of Sema3A molecules inside the vesicle (N_v) was ~2,500. (c) as in a, but in this case the GC, 2 minutes after VB turned away from L_v. (d) as in b but profiles obtained from the GC that are shown in c. In this experiment $N_v \sim 1{,}000$. (e) Time evolution of the distance (*Dist*) between L_v, i.e. the location of the center of the vesicle and the nearest tip of the GC for 5 different experiments. The vertical broken line indicates the time of VB. Following VB the GCs retracted with a delay varying from 20 to 120 s. Scale bar: 5 µm.

dimension, between 10 and 10^4 guidance molecules were encapsulated in lipid vesicles. Vesicles were trapped with an infrared (IR) laser tweezers (see Supplementary Information 1) in front of an exploring hippocampal GC (Fig. 1a). GC navigation was followed by time lapse video microscopy during the entire duration of the experiment. GC navigation was monitored for some minutes and then, using a short UV laser pulse, the vesicle was broken, so guidance molecules could diffuse in the dish reaching the GC membrane. Diffusion of molecules, following vesicle breaking (VB) was verified by loading vesicles with fluorescein and Quantum Dots (see Supplementary Information 2).

Release of guidance molecules induces repulsion or growth in less than 1 minute. Alive and healthy GCs continuously explore the environment (see frames at −60 and −10 s of Fig. 1a). During this exploratory phase, filopodia tips could move by several µm in a minute (Fig. 1b). Having observed the GC exploratory motion, we delivered the UV laser pulse focused on the vesicle, and trapped Sema3A molecules diffused. Following Sema3A release, the GC started to retract within 20–60 s (compare frames at −10 s and at the following times in Fig. 1a). Within 2 minutes the lamellipodium retracted by 1–3 µm and several filopodia completely disappeared (Fig. 1b). From acquired images we measured the distance (*Dist*) between the location of the vesicle (L_v) and the nearest tip of the GC (Supplementary Information 3). Before VB, *Dist* oscillated with a standard deviation σ of 0.5 µm, but after VB, *Dist* significantly increased by 2–5 µm with a delay varying from 20 to 120 seconds (Fig. 1e). When the number of encapsulated Sema3A molecules ranged from 10^3 to 10^4 *Dist* increased (in 49/60 experiments) - from its value measured in a window of 60 seconds before VB - with statistical significance (Wilcoxon test: p=0.03) indicating GC retraction (Fig. 1a and b); in the remaining 11/60 experiments *Dist* did not change significantly but in 6 of them the GC turned away and grew in a different direction with respect to L_v (Fig. 1c and d).

Breaking of the vesicle with a UV laser pulse was determined by major changes in its shape, as confirmed by video microscopy. As previously described[26], we checked whether molecules could remain trapped inside broken vesicles, by encapsulating fluorescence molecules inside vesicles: when the round shape of the vesicle was altered by the UV laser pulse we rarely detected any residual fluorescence.

Subsequently, we encapsulated in the lipid vesicles Netrin-1, an attracting signaling molecule to compare the effect of repellant (Sema3A) and attractant molecules. When vesicles contained a high number of Netrin-1 molecules (N_v>1,500) after VB filopodia grew towards L_v (compare in Fig. 2a and c, frames taken at -10 s and at following times, and the corresponding profiles in b and d). The GC grew towards L_v also when the concentration of Netrin-1 molecules inside the vesicles was 5 times reduced. In 39/70 experiments with a number of Netrin-1 molecules inside vesicles ranging from 10^3 to 10^4 following VB, *Dist* decreased (Wilcoxon test: p= 0.03) indicating a clear attraction. In 24 experiments *Dist* increased significantly (Wilcoxon test: p=0.027) indicating GC repulsion and in 7 experiments we did not observe any significant change of GC navigation. The action of Netrin-1 was as fast as that of Sema3A and initiation of growth could be observed also 20 s after VB (Fig. 2e). These experiments confirmed that Netrin-1 in hippocampal GCs is a bifunctional signaling molecule, evoking both attraction and repulsion[28,29].

When GCs are exposed to glutamate gradients[30] or to chemicals inducing GC turning,[31] filopodia emerging from GCs rearrange quickly: indeed the ratio between near and distant filopodia changes in less than 1 minute following the onset of drug application. These results are in agreement with the fast growth/retraction of filopodia here described, often occurring within 20 seconds after VB.

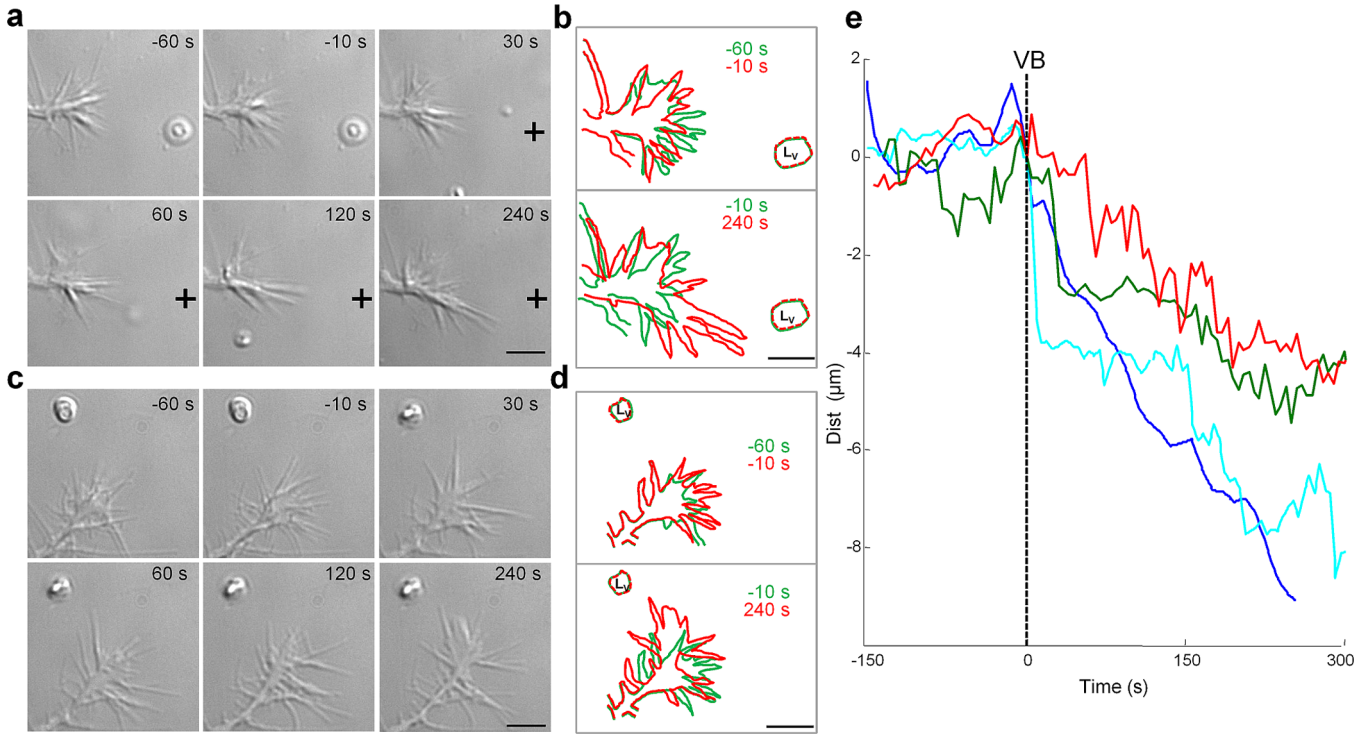

Figure 2 | The release of Netrin-1 from vesicles induces either attraction or turning. (a) DIC images of a GC before VB (−60 s and −10 s) and after VB (30, 60, 120 and 240 s) Black crosses indicate L_v. (b) top: GC profiles at −60 s (green) and −10 s (red) before VB; bottom: GC profiles at -10 s (green) and 240 s (red) after VB. GC before VB explored the environment, but after VB they clearly grew towards L_v . In this experiment the laser pulse completely broke the lipid vesicle. N_v~1,750. (c) as in a, but N_v~950. (d) as in b but profiles obtained from the GC shown in c. (e) Time evolution of the distance (*Dist*) between L_v and the nearest tip of the GC for 5 different experiments. The vertical broken line indicates the time of VB. Following VB the GC started to grow with a delay varying from 20 to 60 s. Scale bar: 5 µm.

When PBS was encapsulated in lipid vesicles positioned in front of an exploring GC, following VB, the GC continued to explore the environment (see Supplementary Information 4). During 1 minute following VB, the number of filopodia that spontaneously appeared or grew by more than 50% was 0.9 ± 0.6 and the number of filopodia that spontaneously retracted by more than 50% was 1.2 ± 0.7 (N=14 experiments).

Effect of breaking vesicles containing a small number of guidance molecules. In previous experiments (Figs 1 and 2) N_v was larger than 1,000. In order to determine the minimum value of N_v necessary to evoke attraction we performed experiments by decreasing the value of N_v and considering only experiments where Netrin-1 was attracting. When the concentration c of guidance molecules inside vesicles is reduced, two factors determine the exact value of N_v: first N_v becomes a random variable following a Poisson distribution[32] and second, the mean value of N_v will depend on the efficiency of the encapsulating procedure, i.e. to what extent the bulk concentration of guidance molecules c is equal to its concentration inside vesicles c_v. As described in the Methods section, by using Quantum Dots we verified that the encapsulation efficiency $\varepsilon = c_v/c$ was approximately equal to 0.35.

When N_v was in the range of 100, following VB, several new filopodia grew and often also a lamellipodium connecting the new filopodia emerged (Fig. 3a). When N_v was decreased to less than 40, only a few filopodia (usually 1 or 2) grew by more than 50 % (Fig. 3b–d). In order to estimate the minimum number of guidance molecules able to modify GC navigation, we counted the number of filopodia ($N_{newfilo}$) that either appeared after VB or grew by more than 50%. The observed values of $N_{newfilo}$ collected from 32 experiments with N_v <140 and the averaged 14 observed values for N_v=0 (control experiments with PBS) (Fig. 3e) show that the relationship between $N_{newfilo}$ and N_v could be fitted by a straight line ($N_{newfilo}$ = a + b N_v) with parameters a=1.24 and b=0.045 (chi-square two-tailed test with significance = 0.05). The slope of this line suggests that the range of Netrin-1 molecules inside vesicles necessary to drive the growth of a single filopodium is approximately 22. This value was confirmed by testing the statistical significance of the differences with the controls (Student t-test, $p<0.05$) .

We repeated similar experiments with vesicles containing Sema3A. When the number of Sema3A molecules inside the vesicle N_v was larger than 2,000, after VB, several filopodia pointing towards L_v quickly retracted (Fig. 4a) within 60 sec. When N_v was between 1,000 and 1,500 only some filopodia retracted after VB (Fig. 4b–c) but when N_v was below 500 we observed filopodia repulsion very rarely (Fig. 4d–f). We counted the number of filopodia ($N_{filolost}$) which either disappeared or retracted by more than 50% following VB. The observed values of $N_{filolost}$ collected from 36 experiments with N_v <1,400 and the averaged 14 observed values for N_v=0 (control experiments with PBS) (Fig. 4g) show that the relationship between $N_{filolost}$ and N_v is fitted by a straight line of parameters a=1.9 and b=0.001 (chi-square two-tailed test with significance = 0.05), suggesting that the presence of about 1,000 Sema3A molecules inside the vesicle is necessary to induce the repulsion of a single filopodium. This value was confirmed by testing the statistical significance of the differences with the controls (Student t-test, $p<0.05$) .

Estimation of the number of molecules reaching the growth cone. After vesicle breaking, N_v guidance molecules diffuse in all directions (see Supplementary Information 2) and only a fraction of them will reach the GC. In order to estimate the number of molecules reaching the growth cones (N_{GC}), trajectories and arrival times of guidance molecules on the GC membrane were studied by 3D Brownian simulations of the stochastic equation

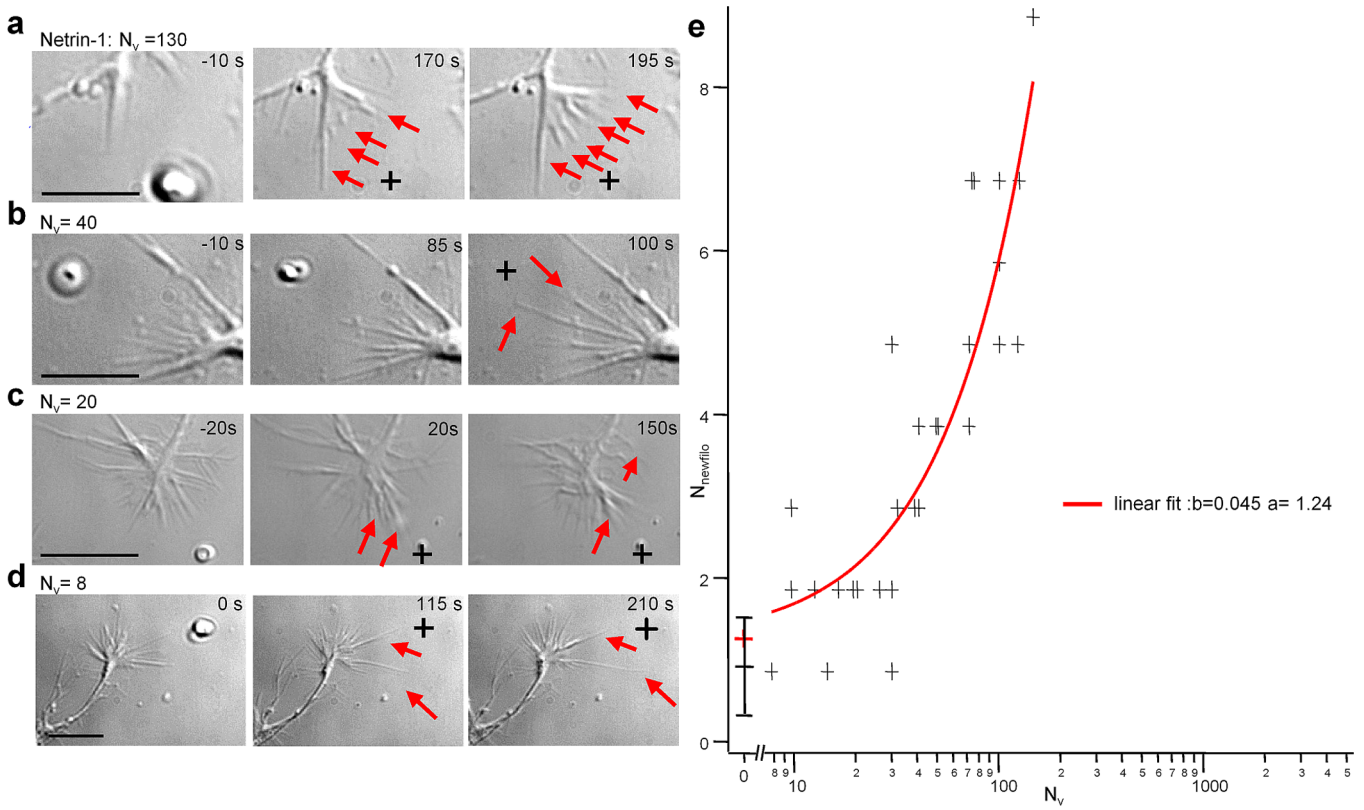

Figure 3 | The release of at least 20 Netrin-1 molecules is sufficient to induce filopodia growth. (a) With 130 Netrin-1 molecules inside the vesicle (N_v=130), after VB several new filopodia grew towards L_v (red arrows).(b) as in a but for N_v=40. (c) as in a but for N_v=20. (d) as in a but for N_v= 8. Black crosses indicate L_v (e) Collected data showing the relation between N_v and $N_{newfilo}$. The least square fit of the experimental data (red curve) with a straight line of parameters a=1.24 and b=0.045 (chi-square two-tailed significance=0.05) suggests that the presence of approximately 22 Netrin-1 molecules inside vesicles are sufficient to drive the growth of a single filopodium. Data were confirmed by statistical significance. Note that the results of N=14 control experiments are illustrated by mean value and dispersion bar. Scale bar: 10 μm.

$$dX_t = \sqrt{6\,D}\,dw_t \qquad X_0 = L_V \tag{1}$$

where dw_t is the differential of the Wiener process[33] and D is the diffusion coefficient with the initial condition L_v = *(0,0,a)*.

We assumed that when Sema3A and Netrin-1 collided with the coverslip, they were not absorbed and were reflected back. As Sema3A and Netrin-1 receptors have a very high affinity for Sema3A and Netrin-1 in the pM range[34,35], the GC membrane was assumed to be a perfectly absorbing surface so that guidance molecules hitting the GC membrane are immediately removed from the system.

The molecular weight (MW) of Sema3A and of Netrin-1 is 65 and 75 kDa respectively and the experimentally measured diffusion coefficient D of proteins with a similar MW ranges from 40 to 120 $\mu m^2\,s^{-1}$ (see Supplementary Information 8). Therefore we performed the numerical simulations with values of D varying in this range. The GC membrane was described as a 3D surface, in which the perimeter is drawn by hand from the frame taken at the time of VB (see yellow profile in Fig. 5a and b), and its height Δz was taken to be Δz = 500 nm. Very fast trajectories reach the GC membrane in less than 100 ms (see Fig. 5a). Trajectories reaching the GC at later times, i.e. 1–10 s after VB, wandered around the GC before hitting it (Fig. 5b). Filopodia emerging from the GC play an important role, because they behave like antennas for guidance molecules and therefore N_{GC}/N_v for GC with many filopodia is higher. By simulating 10,000 diffusion events of eq (1) we obtained the distribution of GC hitting times (Fig. 5c) showing that the first guidance molecules reach the GC membrane within some hundred of milliseconds, and that 90% of the particles hit the GC membrane within 10 s (see Fig. 5d). The ratio N_{GC}/N_v depends on the value of Δz (Fig. 5e), and on the exact shape of the GC. We simulated eq (1) for different shapes and heights of GCs and N_{GC}/N_v varied between 0.06 for values of Δz equal to 100 nm and GC with few filopodia, and was 0.14 for values of Δz about 1 μm and GC with more than 7 filopodia.

The accuracy and quality of numerical simulations were checked by comparing their results with the analytical solution of the corresponding diffusion equations (see Supplementary Information 9).

These simulations suggest that about 10% of the molecules in the vesicle reach the GC membrane within 10 s after VB and therefore N_{GC}/N_v was assumed to be 0.1±0.04. If the value of D had been larger by one or two orders of magnitude, trajectories would have been closed to straight lines not wandering around the GC. In this case N_{GC}/N_v is around 0.01, i.e. close to the ratio $\Omega_{GC}/4\pi$ where Ω_{GC} is the solid angle - in radians - spanned by the GC viewed from the vesicle (see Supplementary Information 10).

Expression of semaphorin and netrin receptors in hippocampal growth cones. Having established that Sema3A and Netrin-1 released from vesicles affect GC navigation, we investigated the expression of their receptors. Hippocampal GCs had a positive staining for Sema3A receptors, neuropilin 1 (NP1) and plexin A1 (PlexA1) after 1 day of culture and the two receptors colocalized (Supplementary Fig. 5).

Netrin-1 receptors composed only of DCC mediate attraction, whereas a complex of DCC and UNC5 mediates repulsion[28,29]. We examined the expression of DCC and UNC5A (known also as UNC5H1) receptors in hippocampal neurons after 1 day *in vitro*. Cells were fixed, permeabilized with 0.1% Triton X-100 and stained with appropriate antibodies. DCC and UNC5A staining appeared

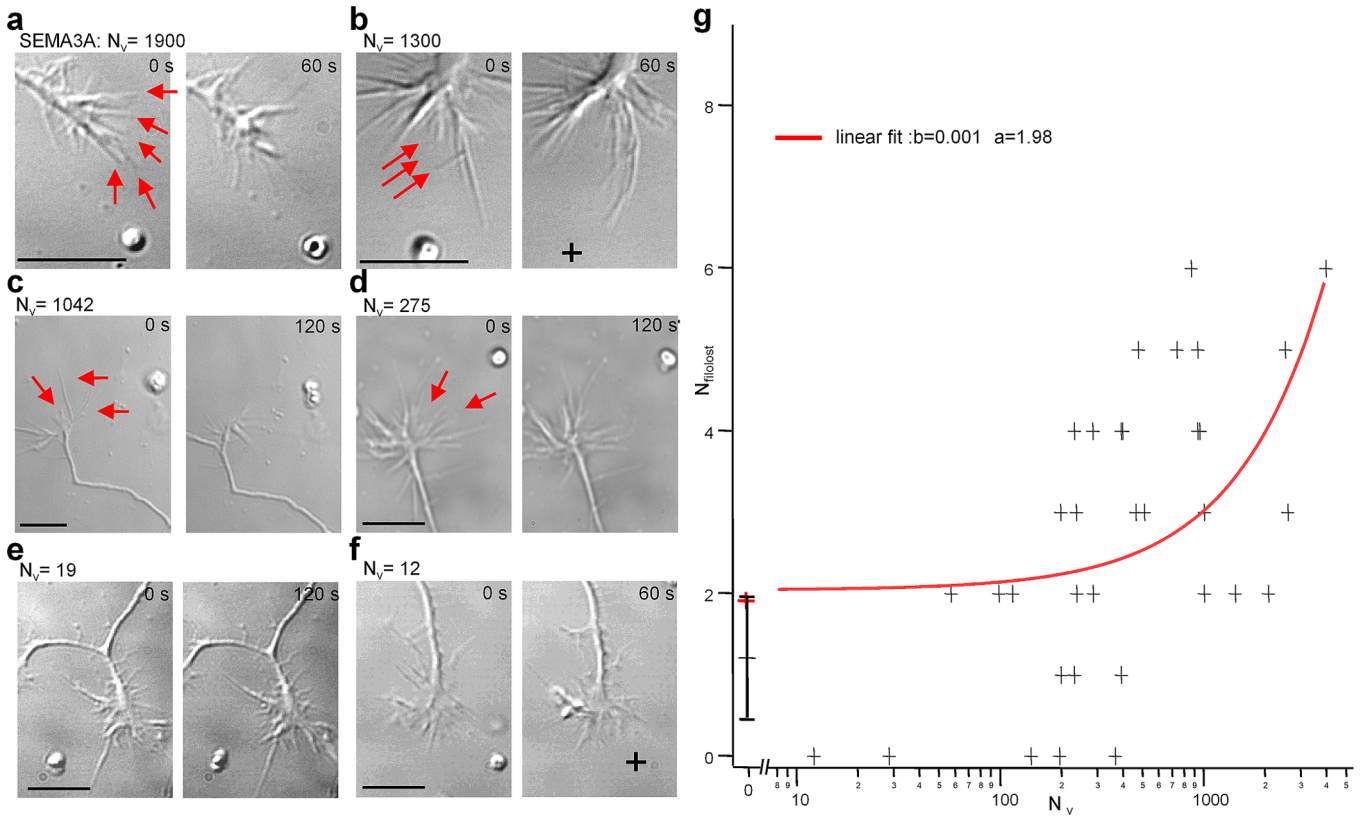

Figure 4 | The release of at least 1000 Sema3A molecules is necessary to induce GC repulsion. (a) For N_v=1900 after VB several filopodia retracted.(b) as in a but for N_v=1,300. (c) as in a but for N_v=1,042. In this case only 1 filopodium clearly retracted. (d), (e) and (f) as in a, but for N_v=275, 19 and 12 respectively. (g) Collected data showing the relation between N_v and $N_{filolost}$. The linear least square fit of the experimental data (red curve) with a straight line of parameters a=1.9 and b=0.001 (chi-square two-tailed significance=0.05) suggests that the presence of approximately 1,000 Sema3A molecules inside the vesicle are necessary to induce the repulsion of a single filopodium. Data were confirmed by statistical significance. Note that the results of N=14 control experiments are illustrated by mean value and dispersion bar. Scale bar: 10 μm.

punctuate[36,37] with a varying degree of colocalization in different GCs. We performed a colocalization analysis using the Volocity 3D imaging software (see Methods). The Pearson's correlation coefficient (PCC) calculated for the GC in Figure 6a–c (see arrows) was 0.19 indicating very low colocalization, while for the GC in Figure 6 d–f the value of PCC was 0.44, indicating a moderate degree of colocalization. In 11/63 GCs DCC and UNC5A did not colocalize (PCC<0.2) and punctae were visible only for DCC (see arrows in Fig. 6c) or UNC5A, separately. In 37/63 GC we observed a moderate colocalization (PCC from 0.2 to 0.5) and in 15/63 GCs we observed a high degree of colocalization of DCC and UNC5A (PCC>0.5) with punctae that stained for both DCC and UNC5A (see arrows in Fig. 6f).

UNC5A, but not DCC, can be removed from the surface of neurons and GCs by endocytosis[13,28,37]. Therefore we excluded the permeabilization with Triton X-100 from the immunofluorescence protocol to analyze the surface expression of UNC5A. In these experimental conditions, half of the GCs (50.78 % ± 2.98, 466 GCs analyzed) were UNC5A-negative (Supplementary Information 6) thus suggesting both membrane and cytoplasmic localization of UNC5A (Supplementary Information 7).

In order to verify whether surface UNC5A-negative GCs mediate attraction in response to Netrin-1, we performed the GC turning assay (see Methods) on neurons grown over a coverslip with a numbered grid allowing the identification of the observed neuron after fixation. GCs were stained with neural cell adhesion molecule (NCAM) and UNC5A without permeabilization with Triton X-100, so to reveal the presence of UNC5A receptors at the cell surface. In these experiments (n=27) a stable Netrin-1 gradient (300 ng/ml) was delivered through a conventional micropipette and after observing attraction or repulsion, neurons were immediately fixed (Fig. 6g–l). The superimposed trajectories of neurite extension during a 45 min period for control PBS (left) and Netrin-1 (right) gradient are shown in Fig. 6h. In this way we verified that GCs attracted by Netrin-1 did not have a positive staining for UNC5A (Fig. 6i–j) while GCs repelled by Netrin-1 were UNC5A-positive (Fig.6 k–l).

Discussion

The results described in the present manuscript are based on a new way of delivering small amounts of guidance molecules in their native form[25,27], in which neither an exogenous light-switchable gate has been inserted[38,39] nor they are attached or cross-linked to a carrier bead[40,41]. In fact properties of caged compounds with a light-switcheable gate are similar but not identical to free compounds: for instance, caged GABA (DPNI-GABA) inhibits $GABA_A$ receptors[42] and caged glutamate (RuBi-glutamate) inhibits GABAergic currents[43].

Our method not only delivers guidance molecules in their native form but also provides an upper bound on the number of guidance molecules reaching the GC and this upper bound can be as small as 5–200. By using this method we have unraveled three major properties of the action of guidance molecules on neuronal GCs: first, the arrival of Sema3A or Netrin-1 on the membrane of hippocampal GCs induces a fast structural rearrangement of the GC cytoskeleton on a time scale of 20 s (Fig. 1 and 2); secondly, the arrival of very few Netrin-1 molecules is sufficient to induce filopodia growth (Fig. 3); thirdly, Sema3A is a less efficient guidance molecule than Netrin-1 and in order to induce filopodia and GC repulsion a higher number of Sema3A molecules need to reach the GC membrane (Fig. 4).

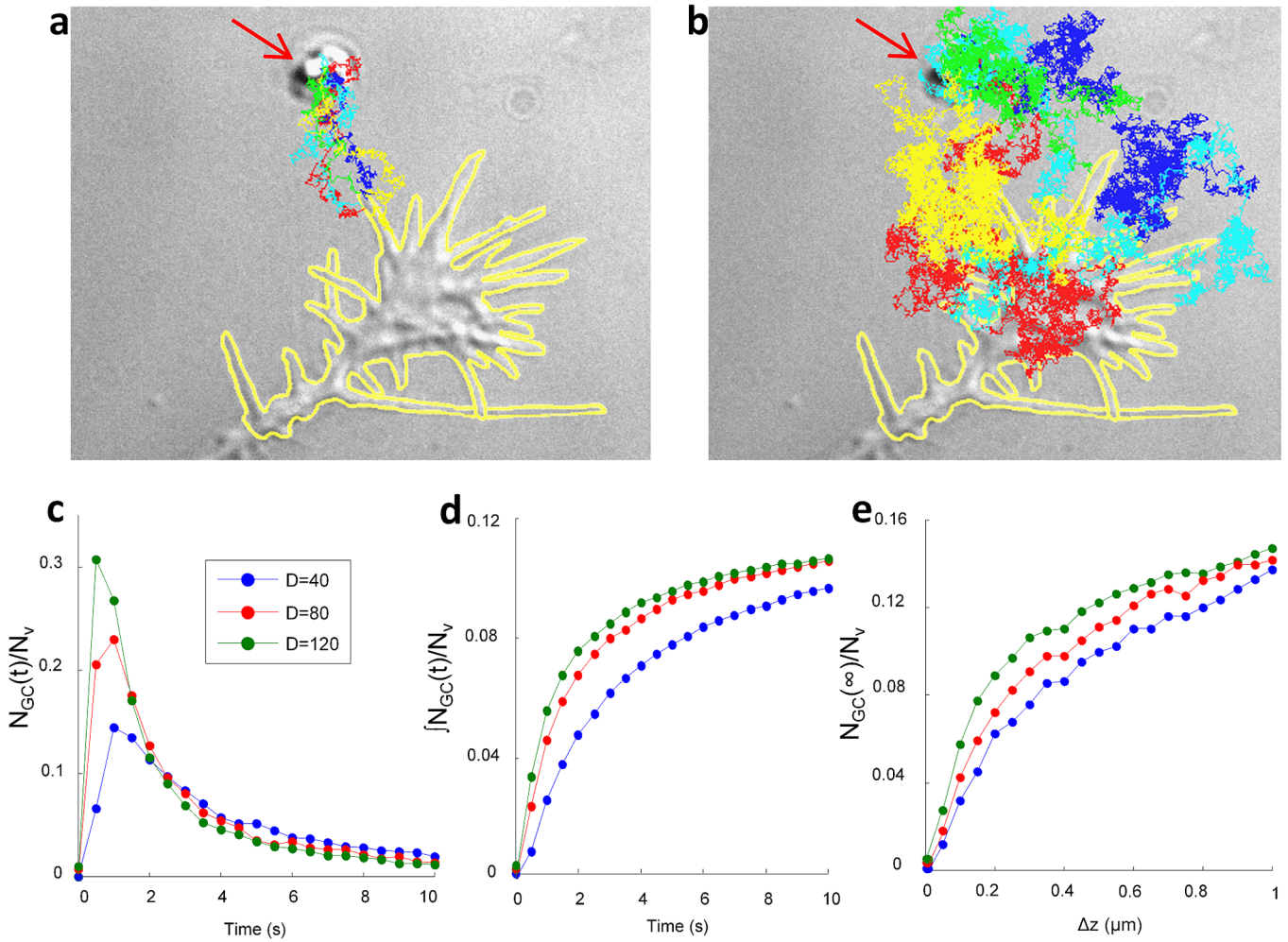

Figure 5 | Estimation of the fraction of released guidance molecules reaching the GC membrane (N_{GC}/N_v). (a) Examples of fast trajectories reaching the GC membrane in less than 1 s after VB. (b) Slower trajectories reaching the GC in 1–10 s after VB. Trajectories were obtained solving the stochastic equation numerically (1) with initial conditions $L_v = (0,0,a)$. The GC profile is shown by the yellow curve. Different trajectories are shown with different colors and the vesicle encapsulating guidance molecules is indicated with the red arrow. (c) Distributions of arrival times on the GC membrane of trajectories starting from L_v for three different diffusion coefficients spanning the considered range. (d) Time integral of the distributions shown in c. (e) The ratio N_{GC}/N_v between the total number of molecules inside the vesicle N_v and those reaching the GC membrane N_{GC} as a function of GC height Δz. These simulations suggest that about 10% of molecules in the vesicle reach the GC membrane within 10 s after VB and N_{GC}/N_v was taken to be 0.1 ± 0.04.

The standard pipette assay[30,31,44,45] provides a simple source of guidance molecules, which has been successfully used in the past and theoretical analysis and direct measurements using fluorescent dyes have shown that, at a distance of some tens of μm from the pipette, the average concentration at the GC can be 10^2–10^3 fold lower than that in the pipette, but it is not possible to determine or even to estimate the order of magnitude of molecules reaching the GC. The Dunn chamber assay[46] and the microfluidic assay[47] provide a better way to control the chemical gradient experienced by the GC, but in these methods, given a constant supply of guidance molecules it is not possible to determine and control the number of guidance molecules reaching the GC in a turning assay. In our experiments guidance molecules were confined in a very limited space and following vesicle rupture it was possible to assess the number of guidance molecules reaching the GC with an error not greater than 60%.

When guidance molecules are released from the vesicle and diffuse in the surrounding medium, they reach the GC membrane - at 3–7 μm away from the initial location of the vesicle - within 1–3 seconds (Fig. 5). Therefore, the delay between VB and cytoskeleton rearrangement is primarily caused by the signaling cascade initiated by Sema3A and Netrin-1 (see Fig. 1e and Fig. 2e). Proteins involved in cytoskeleton rearrangement, such as Rho and Cdc42 are activated in hippocampal spines by glutamate uncaging within 20 s[48], therefore it is not surprising that cytoskeleton rearrangements caused by Sema3A and Netrin-1 can be initiated and even completed within 20 s following VB.

Sema3A[34] and Netrin-1[35] bind to their receptors with a high affinity of 42 nM and 218 pM respectively and when they reach the GC and encounter their receptors they tightly bind to it, activating the corresponding signaling cascade. Collected data (Fig. 3e) of the effect of Netrin-1 can be fitted with a straight line with a slope of about 0.045 $N_{newfilo}/N_v$ suggesting that the presence of 22 Netrin-1 molecules inside a vesicle after VB activates the growth of a single filopodium. Given the error in the estimation of the number of molecules inside vesicles (60%, see Methods) and the experimental variability of obtained measurements a conservative upper bound of the minimum number of Netrin-1 molecules inside a vesicle necessary to initiate neurite growth is 50, i.e. more than twice the value of 22. Filopodia and GC repulsion caused by Sema3A requires the presence inside vesicles of a higher number of molecules, above some hundreds (Fig. 4). Assuming that after VB all guidance molecules are free to diffuse and none of them remains trapped within the lipids,

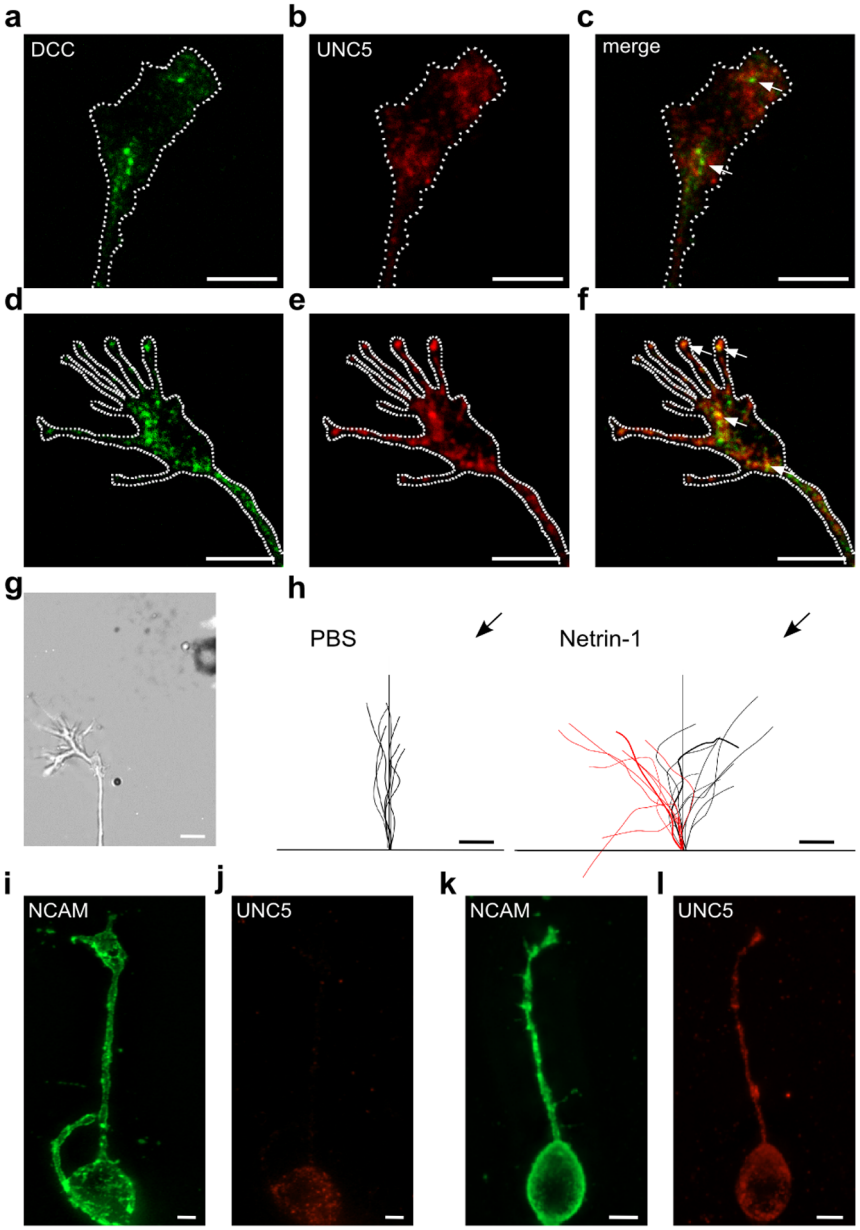

Figure 6 | Hippocampal GCs after 1 day of culture express DCC and UNC5A receptors. (a)–(f): immunostaining of hippocampal GCs with antibodies for DCC and UNC5A. (a) and (d) DCC (green), (b) and (e) UNC5A (red) and (c) and (f) merged confocal fluorescence images. The arrow in c indicates absence of colocalization, in f the arrow indicates colocalization. (g) DIC image of the GC used for the turning assay using a Netrin-1 (300 ng/ml) gradient. (h) superimposed trajectories of neurite extension during exposure of control (PBS, left) and Netrin-1 gradient (right) for 10 UNC5A-positive (red lines) and 10 UNC5A-negative (black lines) neurons. The pipette position is indicated by the black arrow. Thick line trajectories refer to GCs shown in (i–j) and (k–l) respectively. (i) and (j) Fluorescence image of the same GC shown in g, attracted by Netrin-1, stained for NCAM (green) and UNC5A (red), respectively. (k) and (l) Fluorescence image of the GC repelled by Netrin-1 stained as in i and j. Scale bar: 5 μm.

numerical simulations (see Fig. 5) indicate that approximately 10–13% of them will reach the GC membrane within 1–5 seconds. Therefore the arrival on the GC membrane of less than 5 Netrin-1 molecules is sufficient to initiate filopodium growth. In contrast, Sema3A molecules are less efficient and similar considerations suggest that, in order to initiate filopodia repulsion, around 200 Sema3A molecules need to reach the GC. This difference of efficiency of guidance molecules is in agreement with previous observations where a concentration of Sema3A significantly higher than that of Netrin-1 was necessary to modify GC navigation[49].

Hippocampal GCs express Sema3A and Netrin-1 receptors. The two receptors for Sema3A, i.e. NP1 and PlexA colocalized and their activation mediated cytoskeletal retraction: indeed, Sema3A release from vesicles induced retraction or turning in >80% of GCs. In contrast, Netrin-1 receptors DCC and UNC5A had only a moderate degree of colocalization (mean PCC value = 0.37). Netrin-1 is a bifunctional guidance cue and we observed that half of the GCs expressed UNC5A on their membrane, in agreement with the observation that in 56% of GCs, Netrin-1 released from vesicles caused attraction. Moreover, we also observed a cytoplasmic localization of UNC5A[28]. Finally, the GC turning assay demonstrated that the surface of the GCs that are attracted by Netrin-1 are UNC5A-negative while those repelled by Netrin-1 are UNC5A-positive (Fig. 6).

Our results reveal that the signaling cascade initiated by Netrin-1 is very efficient and fast, raising the possibility that the activation of a single Netrin-1 receptor initiates cytoskeleton reorganization.

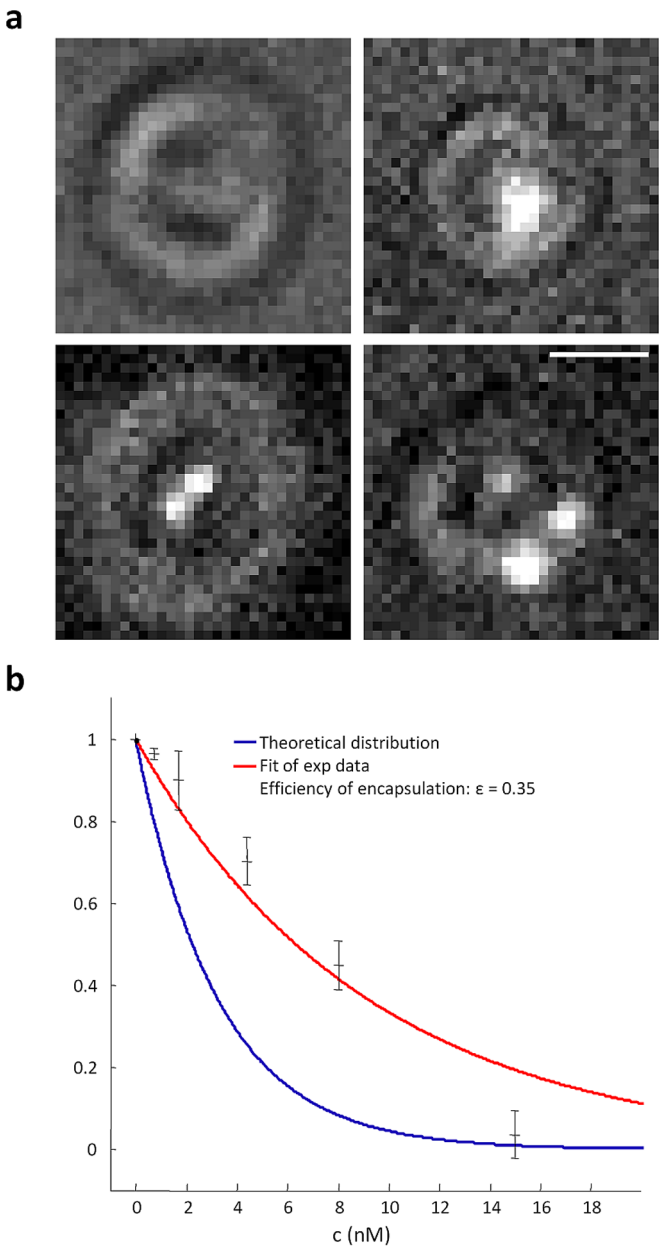

Figure 7 | Quantification of the encapsulation efficiency by QDs analysis. (a) Simultaneous brightfield/fluorescence images of lipid vesicles encapsulating QDs. Due to the diffraction limit on resolution we could not determine the exact number of encapsulated QDs, but we could determine whether a vesicle had QDs inside or not. Therefore we measured the fraction of empty vesicles at different concentrations. (b) Measurement of the fraction of empty vesicles over the total amount of vesicles of 1μm diameter as function of the concentration of QDs. The blue line indicates the theoretical distribution of empty vesicles, while the red line indicates the exponential fit of experimental data giving a value of ε = 0.35. Scale bar: 1 μm.

Signaling by Sema3A is less efficient, requiring the arrival of approximately 40 times more guidance molecules in order to initiate disassembly of the cytoskeleton.

Methods

Vesicle preparation. Vesicles with a diameter of 1–5 μm were obtained with the lipid film hydration method[26] using a hydration solution containing the desired concentration of Netrin-1 or Sema3A. The composition of the lipid mixture was: Cholesterol: 9 μmol, L-α-Phosphatidylcholine: 63 μmol, Stearylamine: 18 μmol (Sigma-Aldrich). The lipid solution was prepared at the concentration of 10 mg/ml in chloroform: methanol (2:1, v/v). The solution obtained was then saturated with nitrogen and stored at −20 °C. Sucrose 100 mM was also included in the hydration solution to allow better vesicle washing and to improve vesicle trapping[50]. After a brief incubation vesicles were formed. Vesicles were then gently centrifuged (5,000 rpm x 3 min) and rinsed 3 times with PBS to wash the external solution. 1–2 μl of the final vesicle solution were then administered to the cell cultures. Single vesicles were subsequently identified, trapped and positioned at the location of interest.

Estimation of the number of molecules in the vesicles. The number of guidance molecules encapsulated in a vesicle (N_v) is a random variable following a Poisson distribution[32] where the probability $P(N_v)$ of having N_v molecules in a vesicle is

$$P(N_v) = \frac{\lambda^{N_v} e^{-\lambda}}{N_v!} \tag{2}$$

where λ is the average number of encapsulated molecules. λ is obtained as the product of the vesicle volume and the concentration (c) of the solution containing Sema3A or Netrin-1 as:

$$\lambda = \pi/6 \; d^3 \; 10^{-15} \mathrm{c} \, N_A \, \varepsilon \tag{3}$$

where d is the vesicle diameter (in μm), N_A is the Avogadro's number and ε is the encapsulation efficiency. Therefore, by varying the concentration c of Sema3A or Netrin-1 and by suitably selecting the dimension of the vesicle we determined the amounts of guidance molecules encapsulated in the vesicles, given the efficiency of the encapsulation procedure.

The encapsulating efficiency (ε) is equal to c_v/c where c_v is the guidance molecule concentration inside vesicles. c_v was evaluated by using solutions of Quantum Dots (QDs). Vesicles were localized using bright field illumination, while QDs were imaged using conventional epifluorescence (Fig. 7a). Light coming from the Hg lamp was filtered with a G-2A filter cube (Nikon) that has a wide excitation bandpass and a longpass emission filter. The high brightness of QDs allowed their visualization even in the presence of low bright field illumination. Vesicles containing QDs could be easily distinguished from empty vesicles, while it was difficult to determine the exact number of QDs inside a vesicle because of diffraction limit resolution. Therefore we measured the percentage of empty vesicles obtained from different QDs concentrations and we compared measured percentages with those expected from the Poisson distribution of empty vesicles

$$P(0,\lambda) = e^{-\lambda} \tag{4}$$

In order to remove the dependence of λ on the vesicle dimension, measurements were restricted to vesicles with a 1 μm diameter. Experimental data were fitted by equation (4) but with a concentration c 35% of the nominal QD concentration (Fig. 7b). The result of our estimation of the encapsulation efficiency was ε = 0.35.

As N_v is a random variable with a Poisson distribution we have

$$N_v = \lambda \pm \sqrt{\lambda} \tag{5}$$

For large values of λ above 100 the contribution to the error of N_v caused by $\pm\sqrt{\lambda}$ becomes negligible and the relative error is:

$$\Delta\lambda/\lambda = 3\Delta d/d \tag{6}$$

caused by the error of the determination of the vesicle diameter d. As the lateral resolution of the microscope is 0.2 μm, Δd/d is 0.2, and Δλ/λ is 0.60. Therefore the relative error on the determination of N_v in a single vesicle is 60% and if the value of N_v determined from eq (3) is 10, the value of N_v varies from 4 to 16.

Quantum Dots. Qdot® 655 ITK™ quantum dots were purchased from Invitrogen (cat. Q21321MP). The dimension of these QDs was 6x12 nm. A stock solution of QDs (8 μM) was prepared in borate buffer 50 mM, pH 8.3. Further dilutions (0.01, 0.7, 1.7, 4.4, 8 and 15 nM) used for the evaluation of the encapsulation efficiency were prepared in PBS.

Neuronal culture preparation. Hippocampal neurons from Wistar rats (P2–P3) were prepared, in accordance with the regulation of the Italian animal Welfare Act, and under the approval of the local veterinary service. Cells were plated at the concentration of 10^5 cells/ml on glass bottom petri-dishes, polyornithine/matrigel precoated in minimum essential medium (MEM) with Earle's salts and GlutaMAX™ supplemented with with 5% fetal calf serum (all form Invitrogen, Life Technologies, Gaithersburg, MD, USA), 0.5% D-glucose, 14 mM Hepes, 0.1 mg/ml apo-transferrin, 30 μg/ml insulin, 0.1 μg/ml D-biotin, 1 mM vitamin B12, and 2 μg/ml gentamycin (all from Sigma-Aldrich, St.Louis, MO). Neuronal cultures were maintained in an incubator at 37°C, 5% CO_2 and 95% moisture and were used after 18–24 hours of culture. Before the experiment, cultures were bathed in Ringer's solution (145 mM NaCl, 3 mM KCl, 1.5 mM $CaCl_2$, 1 mM $MgCl_2$, 5 mM glucose, 10 mM HEPES, adjusted to pH 7.4 with NaOH). During the experiments the dish with hippocampal neurons was kept at 36–37°C by a temperature controller (Temp Control 37-2, PeCon, Erbach, Germany). Experiments with the same dish never lasted longer than 60 minutes. After less than one hour we changed the dish and we repeated our experiments with a new dish. In each dish we performed about 1–2 assays in which we

trapped the vesicle with the optical tweezers and moved it in front of a selected GC. During this time we did not observe any significant evaporation of the liquid and therefore we did not add any liquid. We also performed some control experiments with sealed dishes, i.e. in which a thin coverslip was added at the top to block or reduce evaporation. In these experiments filopodia retracted and grew similarly to what observed in open dishes.

Immunostaining and imaging. Cells were fixed in 4% paraformaldehyde containing 0.15% picric acid in phosphate-buffered saline (PBS), saturated with 0.1 M glycine, permeabilized with 0.1% Triton X-100, saturated with 0.5% BSA (all from Sigma-Aldrich, St.Louis, MO) in PBS and then incubated for 1h with primary antibodies: rabbit polyclonal antibody against DCC (Santa Cruz Biotechnology, Santa Cruz, CA), goat polyclonal antibody against UNC5H1 (Santa Cruz Biotechnology, Santa Cruz, CA) and rabbit polyclonal antibody against neural cell adhesion molecule (NCAM, Millipore, Bedford, MA). The secondary antibodies were donkey anti-rabbit 488 and donkey anti-goat 594 Alexa (Invitrogen, Life Technologies, Gaithersburg, MD, USA) and the incubation time was 30 min. Total nuclei were stained with 2 μg/ml Hoechst 33342 (Sigma-Aldrich, St.Louis, MO) in PBS for 5 min. All the incubations were performed at room temperature (20–22°C). The cells were examined using a Leica DMIRE2 confocal microscope (Leica Microsystems GmbH, Germany) equipped with DIC and fluorescence optics, Diode laser 405nm, Ar/ArKr 488nm and He/Ne 543/594nm lasers. The fluorescence images (1024x1024 pixels) were collected with a 63x magnification and 1.4 NA oil-immersion objective. Leica LCS Lite and Image J by W. Rasband (developed at the U.S. National Institutes of Health and available at http://rsbweb.nih.gov/ij/) were used for image processing. For the colocalization analysis, the laser intensity, exposure, and gain settings per channel were the same for each image, and Volocity 5.4 3D imaging software PerkinElmer, Coventry, UK) was used. The thresholded Pearson's correlation coefficient (PCC) was calculated for all of the voxels in an image pair[51].

GC turning assays. 16–24 hr after culture plating, dissociated hippocampal neurons exhibited active neurite extension. A stable Netrin-1 (R&D Systems, Minneapolis, MN) gradient was created and maintained using a Picospritzer III (Intracel, Royston, UK) ejecting picoliter pulses of Netrin-1 solution (300 ng/ml in PBS supplemented with 0.1% BSA) applied repetitively at a pressure of 7 psi, frequency of 2 Hz and duration 20 ms from a micropipette with 1 μm opening. The micropipette tip was positioned 100 μm from the GC center and 45° from the direction of the neurite extension. Cells were maintained at 37°C and atmospheric CO_2 on a heated stage in a Ringer's solution and examined up to 1 hr after the onset of the Netrin-1 gradient for each coverslip. Cell images were recorded every 60 s. GCs were examined up to 1 hr in a Ringer's solution after the onset of the Netrin-1 gradient in all experiments. In control experiments, PBS alone was ejected from the micropipette. Immediately after recording the last image, cells were fixed with 4% paraformaldehyde containing 0.15% picric acid in PBS for 20 minutes at room temperature (20–22°C) and immunostained. Neurons were cultured on coverslips with numbered grids (Electron Microscopy Sciences, Hatfield, PA) that provided a reference allowing the identification of the tested GCs after fixation.

The trajectory of each neurite for the period of exposure to the Netrin-1 gradient was traced from the video images.

Statistical analyses. All data are shown as means ± s.d. Statistical significance was evaluated using the Wilcoxon test and the chi-square test.

1. Dai, J. & Sheetz, M. P. Mechanical properties of neuronal growth cone membranes studied by tether formation with laser optical tweezers. *Biophys J* **68**, 988–96 (1995).
2. Atilgan, E., Wirtz, D. & Sun, S. X. Mechanics and dynamics of actin-driven thin membrane protrusions. *Biophys J* **90**, 65–76 (2006).
3. Solecki, D. J., Govek, E. E. & Hatten, M. E. mPar6 alpha controls neuronal migration. *J Neurosci* **26**, 10624–5 (2006).
4. Ghashghaei, H. T., Lai, C. & Anton, E. S. Neuronal migration in the adult brain: are we there yet? *Nat Rev Neurosci* **8**, 141–51 (2007).
5. Bray, D., Thomas, C. & Shaw, G. Growth cone formation in cultures of sensory neurons. *Proc Natl Acad Sci U S A* **75**, 5226–9 (1978).
6. Goodman, C. S. Mechanisms and molecules that control growth cone guidance. *Annu Rev Neurosci* **19**, 341–77 (1996).
7. Song, H. & Poo, M. The cell biology of neuronal navigation. *Nat Cell Biol* **3**, E81–8 (2001).
8. Gordon-Weeks, P. R. Microtubules and growth cone function. *J Neurobiol* **58**, 70–83 (2004).
9. Pollard, T. D., Blanchoin, L. & Mullins, R. D. Molecular mechanisms controlling actin filament dynamics in nonmuscle cells. *Annu Rev Biophys Biomol Struct* **29**, 545–76 (2000).
10. Grunwald, I. C. & Klein, R. Axon guidance: receptor complexes and signaling mechanisms. *Curr Opin Neurobiol* **12**, 250–9 (2002).
11. Guan, K. L. & Rao, Y. Signalling mechanisms mediating neuronal responses to guidance cues. *Nat Rev Neurosci* **4**, 941–56 (2003).
12. Huber, A. B., Kolodkin, A. L., Ginty, D. D. & Cloutier, J. F. Signaling at the growth cone: ligand-receptor complexes and the control of axon growth and guidance. *Annu Rev Neurosci* **26**, 509–63 (2003).
13. Bashaw, G. J. & Klein, R. Signaling from axon guidance receptors. *Cold Spring Harb Perspect Biol* **2**, a001941 (2010).
14. Fiore, R. & Puschel, A. W. The function of semaphorins during nervous system development. *Front Biosci* **8**, s484–99 (2003).
15. Livesey, F. J. Netrins and netrin receptors. *Cellular and Molecular Life Sciences* **56**, 62–68 (1999).
16. Dickson, B. J. & Gilestro, G. F. Regulation of commissural axon pathfinding by slit and its Robo receptors. *Annu Rev Cell Dev Biol* **22**, 651–75 (2006).
17. Martinez, A. & Soriano, E. Functions of ephrin/Eph interactions in the development of the nervous system: emphasis on the hippocampal system. *Brain Res Brain Res Rev* **49**, 211–26 (2005).
18. Hong, K. *et al.* A ligand-gated association between cytoplasmic domains of UNC5 and DCC family receptors converts netrin-induced growth cone attraction to repulsion. *Cell* **97**, 927–41 (1999).
19. Masuda, T. *et al.* Netrin-1 acts as a repulsive guidance cue for sensory axonal projections toward the spinal cord. *J Neurosci* **28**, 10380–5 (2008).
20. Hamelin, M. *et al.* Expression of the UNC-5 guidance receptor in the touch neurons of C. elegans steers their axons dorsally. *Nature* **364**, 327–330 (1993).
21. Tojima, T., Hines, J. H., Henley, J. R. & Kamiguchi, H. Second messengers and membrane trafficking direct and organize growth cone steering. *Nat Rev Neurosci* **12**, 191–203 (2011).
22. Lowery, L. A. & Van Vactor, D. The trip of the tip: understanding the growth cone machinery. *Nat Rev Mol Cell Biol* **10**, 332–43 (2009).
23. Chiu, D. T. *et al.* Manipulating the biochemical nanoenvironment around single molecules contained within vesicles. *Chemical Physics* **247**, 133–139 (1999).
24. Rhoades, E., Gussakovsky, E. & Haran, G. Watching proteins fold one molecule at a time. *Proc Natl Acad Sci U S A* **100**, 3197–202 (2003).
25. Sun, B. & Chiu, D. T. Spatially and temporally resolved delivery of stimuli to single cells. *J Am Chem Soc* **125**, 3702–3 (2003).
26. Pinato, G. *et al.* Optical delivery of liposome encapsulated chemical stimuli to neuronal cells. *J Biomed Opt* **16**, 095001 (2011).
27. Pinato, G. *et al.* Neuronal chemotaxis by optically manipulated liposomes. *J Europ. Opt. Soc. Rap. Public.* **6**, 11042 (2011).
28. Bartoe, J. L. *et al.* Protein interacting with C-kinase 1/protein kinase Calpha-mediated endocytosis converts netrin-1-mediated repulsion to attraction. *J Neurosci* **26**, 3192–205 (2006).
29. Moore, S. W., Tessier-Lavigne, M. & Kennedy, T. E. Netrins and their receptors. *Adv Exp Med Biol* **621**, 17–31 (2007).
30. Zheng, J. Q., Wan, J. J. & Poo, M. M. Essential role of filopodia in chemotropic turning of nerve growth cone induced by a glutamate gradient. *J Neurosci* **16**, 1140–9 (1996).
31. Yuan, X. B. *et al.* Signalling and crosstalk of Rho GTPases in mediating axon guidance. *Nat Cell Biol* **5**, 38–45 (2003).
32. Heider, E. C. *et al.* Quantitative fluorescence microscopy to determine molecular occupancy of phospholipid vesicles. *Anal Chem* **83**, 5128–36 (2011).
33. Øksendal, B. K. *Stochastic differential equations: an introduction with applications.* Springer, 2003.
34. Behar, O., Mizuno, K., Badminton, M. & Woolf, C. J. Semaphorin 3A growth cone collapse requires a sequence homologous to tarantula hanatoxin. *Proc Natl Acad Sci U S A* **96**, 13501–5 (1999).
35. Keino-Masu, K. *et al.* Deleted in Colorectal Cancer (DCC) Encodes a Netrin Receptor. *Cell* **87**, 175–185 (1996).
36. Ren, X. R. *et al.* Focal adhesion kinase in netrin-1 signaling. *Nat Neurosci* **7**, 1204–12 (2004).
37. Tcherkezian, J. *et al.* Transmembrane receptor DCC associates with protein synthesis machinery and regulates translation. *Cell* **141**, 632–44 (2010).
38. Ellis-Davies, G. C. Caged compounds: photorelease technology for control of cellular chemistry and physiology. *Nat Methods* **4**, 619–28 (2007).
39. Gorostiza, P. & Isacoff, E. Y. Optical switches for remote and noninvasive control of cell signaling. *Science* **322**, 395–9 (2008).
40. D'Este, E. *et al.* Use of optical tweezers technology for long-term, focal stimulation of specific subcellular neuronal compartments. *Integr Biol (Camb)* **3**, 568–77 (2011).
41. Zhang, X. & Poo, M. M. Localized synaptic potentiation by BDNF requires local protein synthesis in the developing axon. *Neuron* **36**, 675–88 (2002).
42. Trigo, F. F., Papageorgiou, G., Corrie, J. E. & Ogden, D. Laser photolysis of DPNI-GABA, a tool for investigating the properties and distribution of GABA receptors and for silencing neurons in situ. *J Neurosci Methods* **181**, 159–69 (2009).
43. Fino, E. & Yuste, R. Dense inhibitory connectivity in neocortex. *Neuron* **69**, 1188–203 (2011).
44. Guan, C. B. *et al.* Long-range Ca2+ signaling from growth cone to soma mediates reversal of neuronal migration induced by slit-2. *Cell* **129**, 385–95 (2007).
45. Pujic, Z., Giacomantonio, C. E., Unni, D., Rosoff, W. J. & Goodhill, G. J. Analysis of the growth cone turning assay for studying axon guidance. *J Neurosci Methods* **170**, 220–8 (2008).
46. Zicha, D., Dunn, G. A. & Brown, A. F. A new direct-viewing chemotaxis chamber. *J Cell Sci* **99 (Pt 4)**, 769–75 (1991).
47. Joanne Wang, C. *et al.* A microfluidics-based turning assay reveals complex growth cone responses to integrated gradients of substrate-bound ECM molecules and diffusible guidance cues. *Lab Chip* **8**, 227–37 (2008).
48. Murakoshi, H., Wang, H. & Yasuda, R. Local, persistent activation of Rho GTPases during plasticity of single dendritic spines. *Nature* **472**, 100–4 (2011).

49. Ming, G. *et al*. Electrical activity modulates growth cone guidance by diffusible factors. *Neuron* **29**, 441–52 (2001).
50. Ichikawa, M. & Yoshikawa, K. Optical transport of a single cell-sized liposome. *Applied Physics Letters* **79**, 4598–4600 (2001).
51. Barlow, A. L. *et al*. Colocalization analysis in fluorescence micrographs: verification of a more accurate calculation of pearson's correlation coefficient. *Microsc Microanal* **16**, 710–24 (2010).

Acknowledgments

We acknowledge funding from the European Union's Seventh Framework Programme FP7 under Grant Agreement n. 214566 (NanoScale) and Grant Agreement n. 270483 (FOCUS). We thank Manuela Schipizza Lough for carefully reading the manuscript and Micaela Grandolfo for the help with the colocalization analysis.

Author contributions

G.P., D.C., L.T.L. and A.A. performed experiments and data analysis. J.B. and L.T.L. performed immunofluorescence and colocalization analysis. L.T.L. prepared neuronal cultures and performed GC turning assay. G.P., D.C. and E.D. performed QDs measurements. D.C. conceived and coordinated the delivery experiments. V.T. supervised the project and wrote the first draft of the ms, but all authors contributed to the final version of the ms.

Additional information

Supplementary information accompanies this paper at http://www.nature.com/scientificreports

Competing financial interests: The authors declare no competing financial interests.

How to cite this article: Pinato, G. *et al.* Less than 5 Netrin-1 molecules initiate attraction but 200 Sema3A molecules are necessary for repulsion. *Sci. Rep.* **2**, 675; DOI:10.1038/srep00675 (2012).